Annals of Botany **112**: 1003–1014, 2013
doi:10.1093/aob/mct168, available online at www.aob.oxfordjournals.org

ANNALS OF BOTANY
Founded 1887

The tannosome is an organelle forming condensed tannins in the chlorophyllous organs of Tracheophyta

Jean-Marc Brillouet[1], Charles Romieu[2], Benoît Schoefs[3], Katalin Solymosi[4], Véronique Cheynier[1], Hélène Fulcrand[1], Jean-Luc Verdeil[2,5] and Geneviève Conéjéro[5,6,*]

[1]*UMR SPO INRA/SupAgro/UM I,* [2]*UMR AGAP INRA/CIRAD/SupAgro, Montpellier, France,* [3]*EA2160 MMS, LUNAM, University of Le Mans, France,* [4]*Department of Plant Anatomy, Eötvös University, Budapest, Hungary,* [5]*Plate-forme d'Histocytologie et d'Imagerie Cellulaire Végétale (PHIV) and* [6]*UMR BPMP INRA/CNRS/SupAgro/UM II, Montpellier, France*
** For correspondence. E-mail conejero@supagro.inra.fr*

Received: 24 January 2013 Returned for revision: 8 April 2013 Accepted: 10 June 2013 Published electronically: 11 September 2013

• *Background and Aims* Condensed tannins (also called proanthocyanidins) are widespread polymers of catechins and are essential for the defence mechanisms of vascular plants (Tracheophyta). A large body of evidence argues for the synthesis of monomeric epicatechin on the cytosolic face of the endoplasmic reticulum and its transport to the vacuole, although the site of its polymerization into tannins remains to be elucidated. The aim of the study was to re-examine the cellular frame of tannin polymerization in various representatives of the Tracheophyta.
• *Methods* Light microscopy epifluorescence, confocal microscopy, transmission electron microscopy (TEM), chemical analysis of tannins following cell fractionation, and immunocytochemistry were used as independent methods on tannin-rich samples from various organs from *Cycadophyta*, *Ginkgophyta*, *Equisetophyta*, *Pteridophyta*, *Coniferophyta* and *Magnoliophyta.* Tissues were fixed in a caffeine–glutaraldehyde mixture and examined by TEM. Other fresh samples were incubated with primary antibodies against proteins from both chloroplastic envelopes and a thylakoidal chlorophyll-carrying protein; they were also incubated with gelatin–Oregon Green, a fluorescent marker of condensed tannins. Coupled spectral analyses of chlorophyll and tannins were carried out by confocal microscopy on fresh tissues and tannin-rich accretions obtained through cell fractionation; chemical analyses of tannins and chlorophylls were also performed on the accretions.
• *Key Results and Conclusions* The presence of the three different chloroplast membranes inside vacuolar accretions that constitute the typical form of tannin storage in vascular plants was established in fresh tissues as well as in purified organelles, using several independent methods. Tannins are polymerized in a new chloroplast-derived organelle, the tannosome. These are formed by pearling of the thylakoids into 30 nm spheres, which are then encapsulated in a tannosome shuttle formed by budding from the chloroplast and bound by a membrane resulting from the fusion of both chloroplast envelopes. The shuttle conveys numerous tannosomes through the cytoplasm towards the vacuole in which it is then incorporated by invagination of the tonoplast. Finally, shuttles bound by a portion of tonoplast aggregate into tannin accretions which are stored in the vacuole. Polymerization of tannins occurs inside the tannosome regardless of the compartment being crossed. A complete sequence of events apparently valid in all studied Tracheophyta is described.

Key words: Tannosome, organelle, condensed tannins, proanthocyanidins, polymerization, chloroplast, tonoplast, vacuole, Tracheophyta, vascular plants.

INTRODUCTION

Condensed tannins, also called proanthocyanidins, are present in most vascular plants and are thought to play diverse roles. They provide defence against herbivores and pathogens, and protection against UV radiation. These secondary metabolites are polymers of catechins belonging to the vast family of flavonoids. Sucrose gradient sub-cellular fractionation, molecular biology and immunocytochemical approaches have suggested that flavonoids are synthesized from phenylpropanoids by a multienzymatic complex loosely bound to the cytosolic face of the endoplasmic reticulum (Wagner and Hrazdina, 1984; Hrazdina *et al.*, 1987; Burbulis and Winkel-Shirley, 1999; Saslowsky and Winkel-Shirley, 2001). It has been hypothesized that tannin inclusions, viewed by transmission electron microscopy (TEM) in cell suspension cultures and calluses from various gymnosperms (Constabel, 1969; Chafe and Durzan, 1973; Parham and Kaustinen, 1977), also originate from the endoplasmic reticulum. However, since these pioneering reports, no ultrastructural and morphological research has been conducted into the ontogenesis of intracellular tannin-forming elements in terrestrial plants. In particular, no ultrastructural studies of chloroplasts, as the source of all plant aromatics through the shikimate pathway (Herrmann, 1995), have been performed, despite the fact that the synthesis of some flavonoids (Saunders and McClure, 1976; Zaprometov and Nikolaeva, 2003) is known to take place in isolated chloroplasts. Few ultrastructural data have been related to the production of phenolic compounds by the chloroplast. Putative phenolics produced by poorly defined organelles vaguely resembling amyloplasts in *Eucalyptus* ray parenchyma were described by Wardrop and Cronshaw (1962), and chloroplasts in the reproductive organs of *Cornus* by

Juhász *et al.* (1969). Compounds thought to be phenolics, because tests for the presence of proteins, lipids and polysaccharides were negative, were found within the thylakoid lumen from lower epidermal cells of *Nymphaea indica* (van Steveninck and van Steveninck, 1980), leaves of *Haberlea rhodopensis* (Georgieva *et al.*, 2010) and in cotyledons, leaves and fruit peels of a few other species (Keresztes and Sárvári, 2001). However, none of the above-mentioned studies identified the exact nature of the putative phenolics observed in the plastids. More recently, gold immunolabelling showed that three enzymes of the phenylpropanoid and flavonoid pathways, cinnamate-4-hydroxylase (C4H) (Chen *et al.*, 2006), chalcone synthase (CHS) (Tian *et al.*, 2008) and anthocyanidin reductase (ANR) (Wang *et al.*, 2010), were primarily located in the chloroplast of developing grape berries.

Based on these data, a detailed ultrastructural and morphological study was carried out to examine the possible involvement of chloroplasts in the ontogenesis of tannin-forming elements in vascular plants.

MATERIALS AND METHODS

Plant materials

Leaflets from fern (*Dryopteris* sp., Pteridophyta), horsetail (*Equisetum arvense* L., Equisetophyta), *Cycas revoluta* Thunb. (Cycadophyta), *Ginkgo biloba* L. (Ginkgophyta) and persimmon (*Dyospiros kaki* L., Magnoliophyta, Eudicots), petioles from *Chamaerops humilis* L. and stalks from *Saccharum* L. sp. (Magnoliophyta, Monocots), needles from *Pinus sylvestris* L. and scales from *Cupressus macrocarpa* Hartw. ex George Gordon (Coniferophyta), and pistils and fruits from grapevine (*Vitis vinifera* L., Magnoliophyta, Eudicots) were collected in the Montpellier City botanical garden.

Light microscopy

Tannin were visualized after fixation, dehydration and embedding of the tissues in resin (Brillouet and Escoute, 2012) by the dimethylaminocinnamaldehyde (DMACA) technique (Treutter, 1989; Cadot *et al.*, 2006).

Fluorescence labelling

Tannin were visualized by dipping sections from grapevine pistils in 0·01 M phosphate-buffered saline (PBS) containing Oregon Green® 488-conjugated gelatin (Invitrogen, USA; 10 μg mL^{-1}) for 1 h, then washing in PBS (3× 15 min); controls were obtained by applying gelatin onto tannin-free tissues, i.e. young stem from *Hedera helix* L. and leaflet from *Phyllostachis* Siebold & Zucc. sp. (Supplementary Data Fig. S1).

Visualization of chloroplast membrane intrinsic proteins was carried out as follows: sections were dipped successively at 20 °C in the following media: 4 % paraformaldehyde in 0·01 M PBS for 1 h; 0·1 M glycine in PBS for 15 min; PBS (3× 15 min); 5 % bovine serum albumin (BSA) in PBS (blocking buffer, 3 h); anti-Lhcb1 (LHCII type I chlorophyll *a*/*b*-binding thylakoidal membrane protein), anti-TIC40 (translocon complex from chloroplast inner membrane) or anti-TOC75 (translocon complex from chloroplast outer membrane) rabbit antibodies (Agrisera, Sweden; 10 μg mL^{-1} in blocking buffer, overnight at 4 °C); PBS (3× 15 min); and secondary anti-rabbit Alexa Fluor® 633-conjugated IgGs (Invitrogen, USA; 7 μg mL^{-1} in blocking buffer, 1 h). Controls were run (1) with pre-immune rabbit serum instead of primary antibody and (2) with secondary anti-rabbit IgGs only.

Confocal and epifluorescence microscopy

Confocal imaging was performed with a Zeiss Axiovert microscope 200M 510 META fitted with a Plan-Apochromat ×63/1·2 W Zeiss objective. Excitations were obtained for gelatin–Oregon Green with an Ar laser at 488 nm (bandpass 500–530 nm), for antibodies with an He–Ne laser at 633 nm (band pass >650 nm) and for tannins with a 405 nm blue diode (bandpass 505–550 nm). Images were processed by Huygens (http://www.svi.nl/HuygensSoftware), then Image J (http://rsbweb.nih.gov/ij/) software: stacked images (16 bits) were converted to RGB (red, green, blue) stacks, then, after thresholding, converted to HSB (hue, saturation, brightness) stacks; then histograms (hue angle) were expressed for each pixel (as a percentage of total pixels) and fitted with a polynomial. For images acquired in lambda scanning mode, the emission spectra were obtained on sample ROIs (regions of interest) by spectral acquisition (lambda stack, excitation at 405 nm). The detection bandwidth was set to collect emissions from 400 to 750 nm, using an array of 32 photomultiplier tube (PMT) detectors, each with a 10·7 nm bandwidth. The method of linear unmixing was applied with advanced iterative and one residual channel. Epifluorescence imaging was performed with an Zeiss Axiophot microscope [DAPI (4',6-diamidino-2-phenylindole) filter, band-path >470 nm).

Transmission electron microscopy

Specimens were dipped in 50 mM sodium cacodylate buffer (pH 7·0) containing 6 % glutaraldehyde (w/v) (Sironval *et al.*, 1968) and 1 % caffeine (w/v) for 6 h, then treated with 1 % osmium tetroxide (w/v) in water for 1 h. After dehydration, they were embedded in Epon EmBed 812. Sections were stained with 0·2 % Oolong tea (Sato *et al.*, 2008). Ultrathin sections (60 nm) were visualized by an H-7100 Hitachi transmission electron microscope with 75 kV accelerating voltage.

Purification and characterization of tannin accretions

Leaflets (5 g) from *Dyospiros* and *Ginkgo*, and pericarp (5 g) from *Vitis*, were gently ground between two alternately rotating discs equipped with stainless steel grids in 50 mL of cold potassium phosphate buffer (pH 7·2) containing 0·3 M sorbitol, 1 % polyvinylpyrolidonne (mol. wt 40 000 Da), 1 % ascorbic acid and 0·34 % EDTA. After filtration on Miracloth, the slurry was centrifuged (1000 *g*, 20 min, 4 °C), and the supernatant was discarded; the pellet was resuspended in the same buffer, homogenized and centrifuged again. After addition of 15 mL of the same buffer, the pellet was homogenized with a Potter Elvejhem, then centrifuged at 100 000 *g* for 1 h on a cushion (90 mL) of 72 % sucrose (w/v; specific gravity d = 1·268). Chloroplasts were stacked at the interface between buffer and 72 % sucrose, while

green accretions sedimented at the tube bottom; the latter were recovered, frozen in liquid nitrogen then stored at −80 °C.

Condensed tannins were analysed by the phloroglucinol technique according to Michodjehoun-Mestres *et al.* (2009): briefly, accretions were washed with distilled water with repeated centrifugation, after which methanol containing 5 % phloroglucinol, 1 % ascorbic acid and 0·2 N HCl was added. After heating at 90 °C for 6 min, the medium was neutralized with an equal volume of 2 % sodium acetate. The phloroglucinol adducts resulting from the depolymerization were analysed by HPLC-DAD-MS (high-performance liquid chromatography-diode array detection-mass spectrometry). Condensed tannins were also detected qualitatively in tannin accretions by the DMACA technique (Treutter, 1989).

Chlorophylls were spectrophotometrically measured in $CHCl_3$/CH_3OH (2:1) extracts at $\lambda = 666$ nm according to Jodłowska and Latała (2011); results were expressed as chlorophyll *a* equivalents.

RESULTS

Examination of tannin-containing cells by electron, light, epifluorescence and confocal microscopy, and biochemical characterization of tannin-containing bodies

For this study on the polymerization of tannins in plants, very young chlorophyllous organs (pistils, immature small fruits, leaflets and pedicels), in which the rate of formation of tannins is highest, were selected (Cohen *et al.*, 2012). The study was first conducted on *V. vinifera*, then extended to plants from other divisions in the Tracheophyta [Cycadophyta, Ginkgophyta, Equisetophyta, Pteridophyta, Coniferophyta, and Magnoliophyta (Eudicots and Monocots)].

Sections from pistils of *V. vinifera* were examined by TEM, and circular osmiophilic and finely granular structures (Fig. 1A) were observed in the vacuole of tannin-containing cells. After specific staining of flavan-3-ols with DMACA, sections obtained from the same materials revealed in light microscopy numerous blue-green stained spheres inside the vacuole (average diameter 0·5 μm) (Fig. 1B). When fresh sections of the same materials were observed in epifluorescence with a DAPI filter, the vacuole appeared as containing several spherical accretions (diameter 3 μm) intensely fluorescing (blue) and including numerous corpuscles (diameter 0·5 μm) emitting the red fluorescence of chlorophyll (Fig. 1C; see also Fig. 3G, H). These chlorophyllous bodies must not be confused with chloroplasts which exhibited far larger sizes and an ellipsoidal (non-spherical) morphology (long axis 2–3 μm, short axis 1–2 μm) (Supplementary Data Fig. 2).

Since there was no method for visualizing tannins specifically, as the DMACA technique detects both monomeric flavan-3-ols and condensed tannins, a technique was developed based on the unique property of tannins to form insoluble complexes with proteins (Hagerman and Butler, 1981). Gelatin coupled to Oregon Green, a fluorophore excitable at 488 nm, was applied to fresh sections of the same materials, and small fluorescing spheres (diameter 0·5 μm) aggregated in a roughly circular accretion (diameter approx. 10 μm) (Fig. 1D–F) were observed in confocal microscopy; image analysis of the merged processed image (Fig. 1G) revealed a continuum between almost-red and tannin-filled almost-green spheres (Fig. 1H). Noticeably, pure red or green spheres were not observed. The gelatin–Oregon Green fluorescent probe did not show non-specific adsorption onto other organelles, membranes or cell walls (Supplementary Data Fig. 1).

With the aim of further characterizing the mixed (tannins/chlorophyll) bodies, they were purified from several organs of diverse plants through high speed centrifugation on a 72 % (w/v) sucrose cushion (Fig. 2A). Abundant chloroplasts were stacked at the (buffer–sucrose) interface, while most, if not all the DMACA-reactive material sedimented at the bottom of the tube, i.e. at a specific gravity >1·268. (Fig. 2A). These elements showed the same typical pattern as that observed on fresh tissue slides under epifluorescence examination (compare Figs 1C and 2A). These heavy elements were subjected to biochemical analyses of condensed tannins and chlorophyll. Compositional analyses confirmed the presence of condensed tannins (Fig. 2B) of various chemical structures according to the division and genus of origin (Table 1): *Ginkgo* tannins were almost exclusively made of epigallocatechin while *Vitis* tannins were mainly constituted of epicatechin; *Dyospiros* tannins were built with a mixture of epigallo- and epicatechin, and they were highly galloylated, in contrast to *Ginkgo* tannins which were not. Their degrees of polymerization were in the range of 10–30 monomers. The starter and extension units were of the same nature in *Ginkgo* and *Dyospiros*, in contrast to *Vitis* where catechin was the terminal unit. Chlorophylls were also present in diverse relative proportions to tannins.

An examination of these purified heavy species by spectral analysis revealed particles (diameter 0·5 μm) exhibiting a double autofluorescence emission spectrum (Fig. 3A–D): a large emission range with several maxima in the 500–600 nm range, typical of condensed tannins (Fig. 3E, F), as well as chlorophyll autofluorescence with the characteristic maximum of photosystem II (λ_{em} 685 nm; Franck *et al.*, 2002). Depending on the plant of origin (*Ginkgo* or *Vitis*) and within the same population of particles, relative proportions of both signals were variable, suggesting a progressive filling of these chlorophyllous bodies with tannins. Coming back to a native tissue (*Vitis* pericarp), the same observations were carried out on minute vacuolar entities (diameter 0·5 μm) (Fig. 3G, H); chloroplasts, as expected, showed the chlorophyll signal only.

Examination of tannin-containing cells by TEM

It should be remembered that, in TEM, all simple phenolics (e.g. quercetin glycosides, chlorogenic acids, and flavan-3-ols such as epicatechin) are solubilized in water–ethanol mixtures and then dehydrated prior to resin embedding; thus, osmiophilic materials observed are the remnants of condensed tannins which have not undergone solubilization due to their complexation with caffeine (Mueller and Greenwood, 1978).

Explants from pistils or very young fruits (diameter 1 mm) were observed by TEM. Functional ellipsoidal chloroplasts (long axis 2–3 μm, short axis 1·5–2 μm) were visible with well-constituted grana thylakoids and the two well-preserved enveloping membranes (Fig. 4A). Other forms of differentiating chloroplasts were observed (Fig. 4B): they were characterized by a swelling with a tendency to circularization [a decrease of the (long/short axis) ratio] and by an unstacking of grana. Unstacked thylakoidal lamellae were slightly swollen and included osmiophilic material that appeared as black spots and dark grey deposits in these inflated zones. Furthermore, these

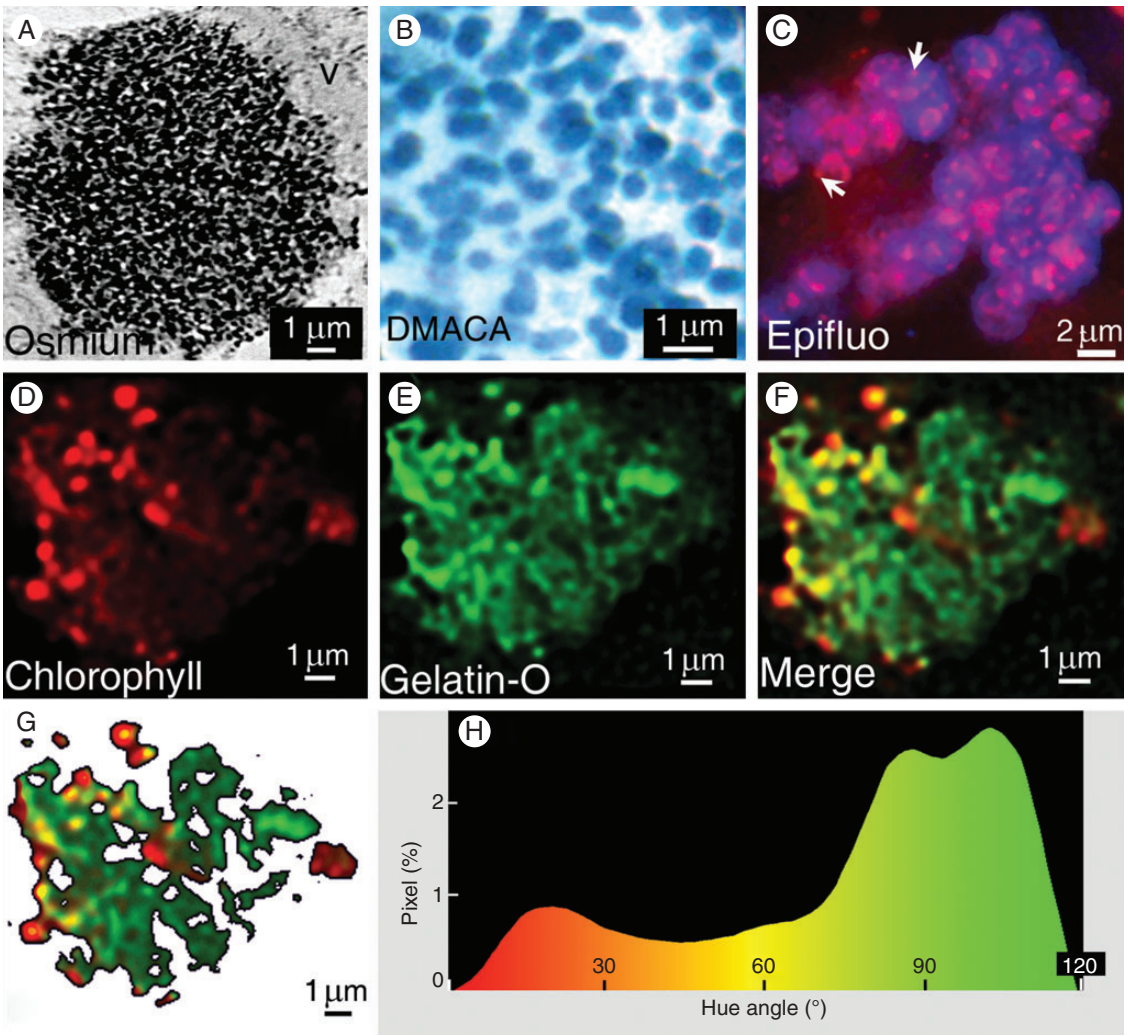

FIG. 1. (A) TEM image of a *Vitis* fruit cell showing a granular osmiophilic cluster of particles (diameter 0·5 µm) in the vacuole. (B) DMACA staining of vacuolar tannins viewed under a light microscope as green-blue particles (diameter as in A). (C) Epifluorescence micrograph (DAPI filter) of chlorophyllous particles (white arrows) embedded in diffuse blue fluorescence of tannins and aggregated into large pseudo-spherical accretions (diameter range 2–20 µm); note the autofluorescence of chlorophyll (fuschia red, i.e. red + blue) and tannins (blue). (D–F) Confocal images of clustered particles (diameter range as in A, B) in the vacuole showing (D) chlorophyll autofluorescence, (E) fluorescence of gelatin–Oregon Green bound to tannins and (F) merged images. (G, H) Image analysis of the merged image (F) after thresholding (G), showing in (H) for each pixel (as percentage/total pixels), its hue angle (°).

lamellae emitted grossly circular structures (diameter 30 nm), including black spots, from their ends into the stroma. Differentiation continued with a massive redistribution of thylakoidal lamellae (Fig. 4C) which seemed shorter and interlaced; some still contained osmiophilic spots and deposits, while others appeared empty. Furthermore, on half of the chloroplast circumference, both enveloping membranes were no longer visible and were replaced by a diffuse cotton-like mass within which were observed osmiophilic spheres which seemed to be expulsed from the interior of the chloroplast; these spherical structures will hereafter designated as 'shuttles'. When examining one of these differentiating chloroplasts through a transverse section (Fig. 4B, D), it was observed that unstacking of grana was accompanied by a whirling of these membranes upon themselves.

Careful examination of the periphery of these chloroplasts showed budding, where part of the inner plastidial content was encapsulated in an emerging structure projected into the cytosol (Fig. 4E): this vesicular structure contained portions of thylakoidal lamellae swollen at regular intervals including osmiophilic spots attached to the inner face of the membrane, in addition to circular structures (diameter 30 nm). These shuttles travelled in the cytosol, after having been emitted from the inner plastidial region (Fig. 4F): two possibly coalescing shuttles may be seen on this micrograph, with one shuttle showing circular structures (diameter 30 nm) with black spots, whereas the other is filled with similar circular structures themselves filled with osmiophilic material. Figure 4G shows a well-delineated full shuttle within the cytosol.

Careful re-examination of the structures generated by the unstacking of grana thylakoids and incorporated into shuttles (Fig. 4H, I) showed that these lamellae, swollen to a greater or lesser degree, were sectioned at regular intervals into small spheres (diameter 30 nm) which progressively filled with

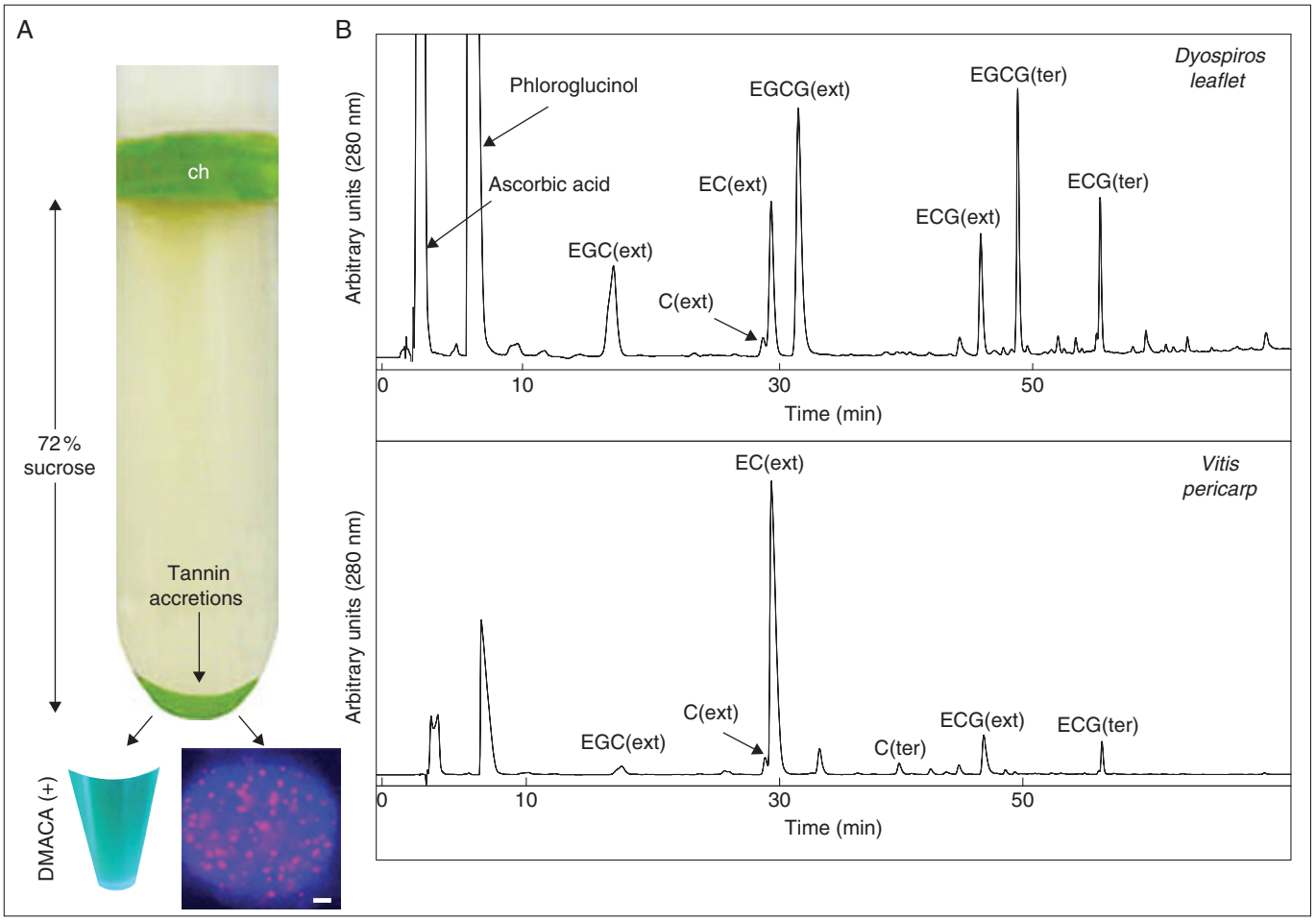

FIG. 2. Purification and characterization of tannin accretions. (A) High speed centrifugation (100 000 *g*) of a *Vitis* extract on a 72 % sucrose cushion: chloroplasts (ch) were stacked at the top of the sucrose cushion while chlorophyllous tannin accretions sedimented at the tube bottom. Accretions showed a positive reaction with DMACA and were observed by epifluorescence microscopy (DAPI filter) as those seen in Fig. 1C (bar 2 μm). (B) Typical HPLC chromatograms of phloroglucinol adducts from condensed tannins present in tannin accretions from *Dyospiros* leaflet and *Vitis* pericarp.

osmiophilic material. The central osmiophilic mass is attached to the inner face of the membrane through a small pedicel (Fig. 4I, yellow arrowhead). These structures, henceforth referred to as 'tannosomes', were also observed entirely filled and with a very regular 30 nm diameter (Fig. 4J).

It was observed that the shuttles ended their journey in the cytosol by penetrating into the vacuole: some contained empty or filling tannosomes and swollen thylakoids (Fig. 5A, C, D) and others even contained a complete thylakoidal system generating tannosomes (Fig. 5B). It was clearly seen that when a shuttle penetrates into the vacuole, it wraps itself in a portion of tonoplast (Fig. 5B, insert), entrapping a corona of cytosol between the tonoplast and the shuttle membrane. This is particularly visible in Fig. 5E showing a shuttle having just passed into the vacuole in which some tannosomes have started accumulating osmiophilic material. Figure 5F–H shows tannosomes in shuttles progressively filling until their inner volume is completely darkened as in Fig. 1A.

Finally, antibodies raised against epitopes from three intrinsic membrane proteins of the chloroplast, LHCII type I chlorophyll *a*/*b*-binding (Lhcb1) (Fig. 6A), and translocon complexes from the inner and outer envelope membranes, (TIC40, and TOC75, respectively) were applied on fresh sections of pistil from *Vitis* (Fig. 6D, G, respectively); autofluorescence of tannins was also observed under confocal microscopy (Fig. 6B, E, H). In all cases, and similarly to what was viewed in Fig. 1D–H, small spheres (diameter 0·5 μm) were observed. These spheres exhibited markings of different intensities against the above-mentioned proteins; the more intense the marking, the lower the amount of tannins present. Image analyses of merged images (Fig. 6C, F, I) revealed a continuum between almost-green and tannin-filled almost-blue spheres (Fig. 6J, K, L). Noticeably, pure green or blue spheres were not observed. This not only confirms the presence of membranes of thylakoidal origin containing chlorophyll in addition to tannins in shuttles, but it also suggests a fusion of chloroplast envelope membranes during their ontogenesis by budding off from the chloroplast. Similar images were obtained with purified tannin accretions (data not shown). The entire data set clearly indicates that the spheres seen in Figs 1B, D–F and 6 are tannin shuttles in the vacuole.

The ontogenesis of the tannosome, a chlorophyllous organelle, achieving the polymerization of condensed tannins, and that of the shuttle ensuring their transport into the vacuole, are presented in Fig. 7.

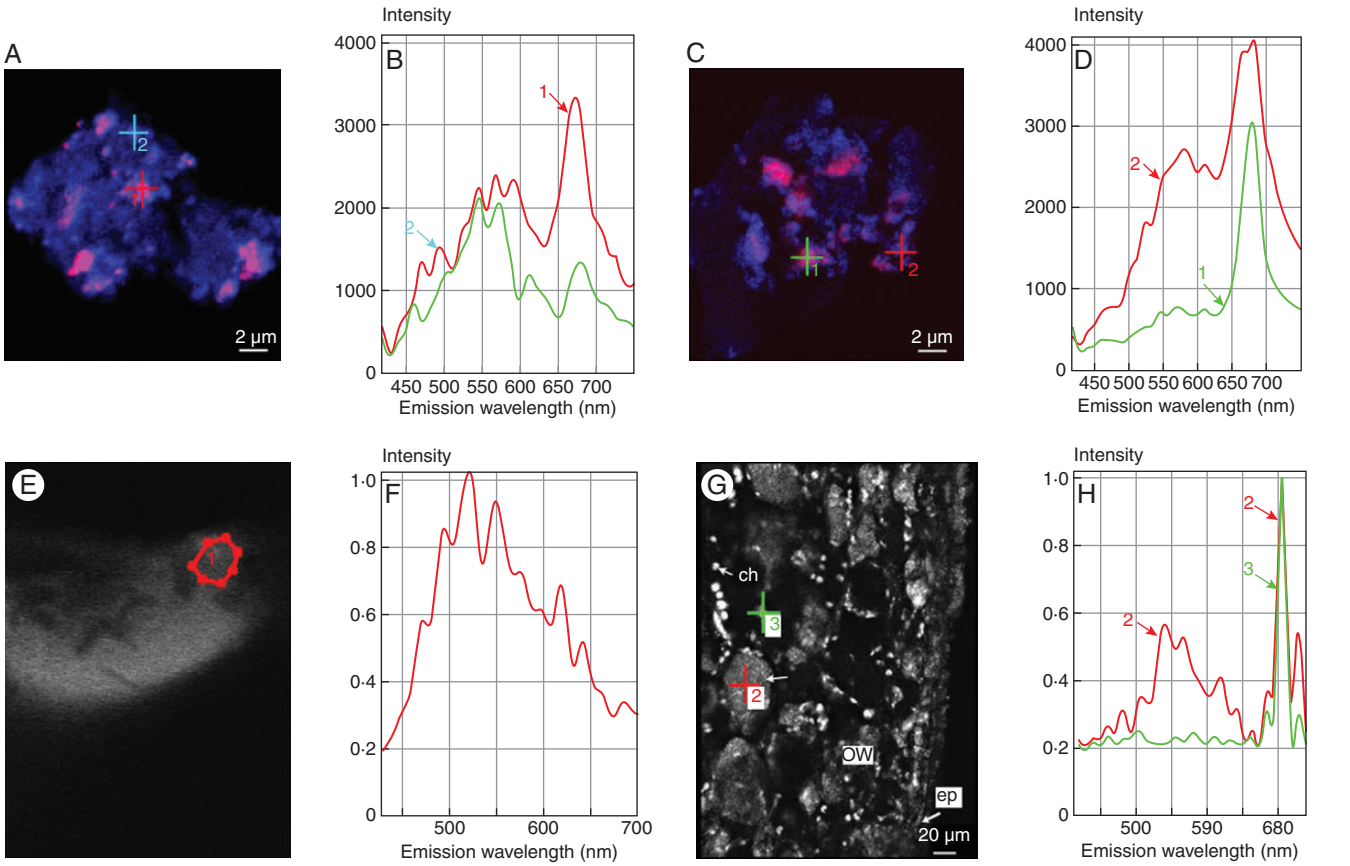

FIG. 3. Subcellular localization of chlorophyll and tannins in *Vitis* and *Ginkgo*. (A, B) Confocal image and spectral analysis of purified *Vitis* tannin accretions showing (1, 2) the chlorophyll emission spectrum (λ_{em} 685 nm) in addition to increasing autofluorescence of tannins (λ_{em} 500–650 nm range). (C, D) Confocal image and spectral analysis of purified *Ginkgo* tannin accretions showing (1, 2) the same phenomenon. (E, F) Confocal image and spectral analysis of grapevine tannins; (1) region of interest. (G, H) Confocal image and spectral analysis of the outer region of a *Vitis* pistil showing (2) vacuolar clusters of chlorophyllous tiny spheres exhibiting fluorescence of tannins and (3) photosynthetic chloroplasts. Abbreviations: ch, chloroplast; ow, ovary wall; ep, epidermis.

Examination of sections from different organs taken from tannin-producing plants from diverse botanical divisions showed, in all cases, the existence of shuttles containing tannosomes similar to those observed in *Vitis* (Supplementary Data Fig. S3). Moreover, as seen in Fig. 1C, groups of shuttles exhibiting the double fluorescence of chlorophyll and condensed tannins similar to those observed in *Vitis* were seen in all the tested Tracheophytes (Supplementary Data Fig. S4). When exhaustively examining sections from tannin-free plant materials (e.g. *H. helix* young stem or *Phyllostachis* leaflet), shuttles were never observed whatever the tissue concerned.

DISCUSSION

Light, epifluorescence and spectral confocal microscopy, and direct chemical analysis, showed that remnants of the chloroplast membranes, including chlorophylls, are intimately associated with tannins, in the large electron-dense accretions representing the final stage in the accumulation of proanthocyanidin polymers within plant vacuoles. Such an association was validated on purified accretions from distant Tracheophytes exhibiting different tannin structures. Ontogenesis of these accretions was described in detail by TEM, confirming their plastidial origin.

Ontogenesis of tannin-forming structures in the present model

The first signs of chloroplast differentiation leading ultimately to the production of condensed tannins are a moderate inflation of the plastid, and an unstacking and slight swelling of the grana thylakoids, similar to those triggered by UV stress in plants (He *et al.*, 1994; Selga and Selga, 1998; Kostina *et al.*, 2001). It should be pointed out that UV-B is a well known upregulator of phenolic biosynthesis (Jansen *et al.*, 1998; Berli *et al.*, 2011). Simultaneously, or soon afterwards, osmiophilic material emerges in the thylakoidal lumen; such dark intralumenal deposits were designated as phenolics without further characterization in a variety of plants and tissues (Juhász *et al.*, 1969; Chafe and Durzan, 1973; van Steveninck and van Steveninck, 1980; Keresztes and Sárvári, 2001; Georgieva *et al.*, 2010). Another symptom is a whirling of thylakoids upon themselves: again, Selga and Selga (1998; Fig. 2A) observed such a phenomenon in the mesophyll of tomato leaf irradiated with excess UV-A. The thylakoids then begin to pearl, generating tannosomes.

These organelles are then encapsulated in shuttles, resulting from the budding off from the chloroplast with fusion of both plastid envelopes. Striking images of plastids expelling membrane-bound vesicles directly into the vacuole with inward folding of the tonoplast were published by Gifford and Stewart

TABLE 1. *Composition of isolated tannin accretions (proanthocyanidins; μmol)**

	Dyospiros kaki: Leaflet	*Ginkgo biloba*: Leaflet	*Vitis vinifera*: Pericarp
Extension units			
Epigallocatechin (EGC)	0·665	2·274	0·722
Epigallocatechin 3-*O*-gallate (EGCG)	0·125	–	–
Catechin (C)	0·024	0·006	0·203
Epicatechin (EC)	0·183	0·127	4·874
Epicatechin 3-*O*-gallate (ECG)	0·034	–	0·163
Terminal units			
Epigallocatechin (EGC)	–	0·071	–
Epigallocatechin 3-*O*-gallate (EGCG)	0·065	–	–
Catechin (C)	–	–	0·148
Epicatechin (EC)	–	0·006	–
Epicatechin 3-*O*-gallate (ECG)	0·030	–	0·069
Molar ratio to epicatechin	EGC/EGCG/EC/ECG 3·64:1·04:1·00:0·35	EGC/EGCG/EC/ECG 17·92:0·00:1·00:0·00	EGC/EGCG/EC/ECG 0·15:0·00:1·00:0·05
Mole per cent of galloylated units[†]	22·6	0·0	3·8
Mole per cent of trihydroxylated units[‡]	75·9	91·6	11·7
Mean degree of polymerization[§]	11·9	32·4	28·4
Total chlorophylls ($\mu g\ mg^{-1}$ tannins)	12·7	4·6	3·4

* Total micromoles in the pellet from ultracentrifugation.
[†] (Σ galloylated units/Σ all units) × 100.
[‡] (Σ units trihydroxylated on the B ring/Σ all units) × 100.
[§] (Σ all units/Σ terminal units).

(1968, figs 17–19) *on Bryophyllum* and *Kalanchoe* (for comparison, see Fig. 5B–D). Finally, the vesicle bound by its membrane and a fragment of tonoplast pinched off at its base was completely released as a vacuolar inclusion (see Fig. 5E). Thus, it is tempting to identify their vesicles with shuttles. These authors mentioned that inclusions could be phenolics on the basis of $FeCl_3$ staining; they also stated that the inclusion could, additionally, contain lipids. The presence in the inner volume of shuttles of numerous tannosomes bound by thylakoidal lipoproteic membranes is consistent with their observations. These vacuolar shuttles which later coalesce into vacuolar tannin accretions were designated as 'complex bodies called coarcervates or aggregates of catechol materials . . . ' (i.e. *ortho*-diphenols) bound by 'a precipitation membrane' by Reed and Dufrénoy (1942) in zinc-deficient apricot leaves. Mueller and Beckman (1976) reported in their work on phenolic-storing cells in cotton plants that no positive origin for the phenolic material could be detected in TEM; nonetheless, their fig. 12 shows small vacuoles containing black particles (diameter 20 nm) which could well account for tannosomes, not to be confused with surrounding free ribosomes. Chafe and Durzan (1973; figs 7, 8) described the proliferation of 30 nm membrane vesicles within a small tannin-containing vacuole in cell suspension cultures of white spruce: again, these vesicles were of the same size as the tannosomes described herein, of too small a diameter to be reticulum-derived vesicles. Whatley (1971, plates 2 and 4, figs 6 and 2, respectively) reported the occurrence of irregularly spaced highly osmiophilic deposits along the outer chloroplast membrane (diameter 0·1 μm) in *Equisetum telmateia* leaves; they may be compared with osmiophilic shuttles observed in Fig. 4B, C. Similar deposits were observed in cold-grown *Brassica napus* (Stefanowska *et al.*, 2002; fig. 2A). More recently, Abrahams *et al.* (2003; fig. 6D) described osmiophilic globules in the endothelium of the arabidopsis *tds-4-1* mutant which upon magnification were built of many smaller aggregate vesicles (diameter 15 nm): these vesicles, which were not commented on further, may well, according to their aggregation into 0·2–2 μm globules, account for tannosomes packed into shuttles. Although morphologically similar to autophagosomes (Kilonsky, 2005), lomasomes and plasmalemmasomes (Marchant and Moore, 1973), the ontogenesis of the tannosome shuttle clearly differentiates it from these sub-compartments.

Finally, chemical analysis unambiguously revealed that dense tannin accretions, purified by sucrose density ultracentrifugation, contained both chlorophylls and condensed tannins of similar structure to those present in integral tissues (Souquet *et al.*, 1996). Taken together, these data unambiguously demonstrate a plastidial origin of tannin polymers.

Tannosomes and their tannosome shuttle hosts were observed in chlorophyll-containing parts of several Tracheophyta from diverse divisions. Therefore, it can be concluded that the formation of tannins by tannosomes is widely distributed among Tracheophyta.

The accepted vs. new model

The current model for the synthesis of the C6–C3–C6 flavonoid skeleton is based on the existence of a multienzymatic complex loosely bound to the rough endoplasmic reticulum

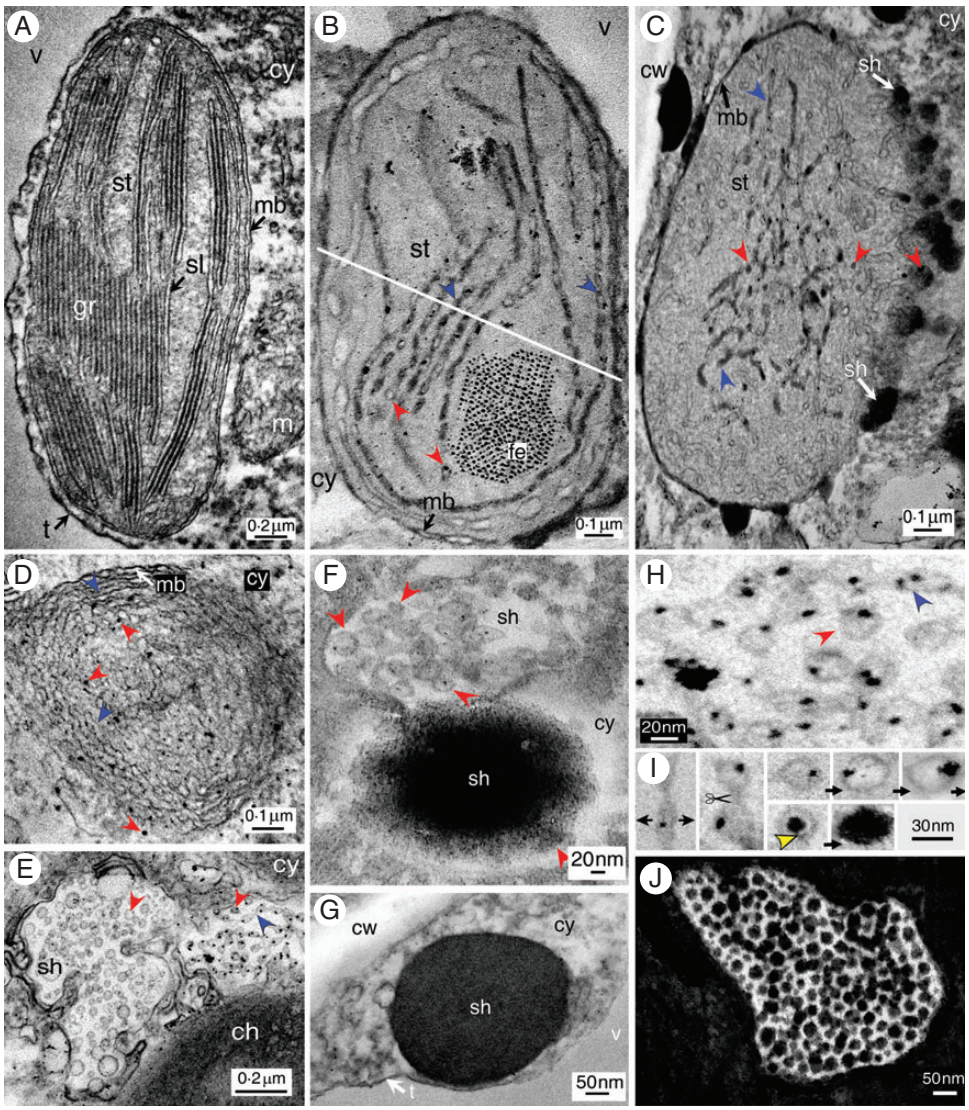

FIG. 4. TEM image of (A) a chloroplast with stacked thylakoids (granum). (B) A differentiating swollen chloroplast with unstacked pearling thylakoids (black-lined blue arrowheads) emitting vesicles (red arrowheads), the tannosomes, at their ends (white line for transverse section). (C) A differentiating chloroplast emitting tannosome shuttles into the cytoplasm. (D) Transverse section of a differentiating chloroplast showing pearling thylakoids wound on themselves. (E) Budding off from a chloroplast of a tannosome shuttle containing pearling thylakoids and tannosomes. (F) Two coalescing tannosome shuttles travelling in the cytoplasm and showing either empty or filled tannosomes. (G) A filled tannosome shuttle in the cytoplasm. (H) Magnified view of pearling thylakoids and their derived tannosomes with one or several osmiophilic grains bound to the inner side of their membrane. (I) Time sequence of the ontogenesis and filling of the tannosome from the thylakoids in a *Vitis* cell; note the yellow arrowhead showing attachment of the osmiophilic deposit through a pedicel to the inner face of the membrane. (J) Very regular distribution of full tannosomes in a shuttle. Abbreviations: cy, cytoplasm; fe, ferritin; m, mitochondrion; mb, outer and inner chloroplast membranes; sh, shuttle; sl, stromal lamella; st, stroma; t, tonoplast; v, vacuole.

(Wagner and Hrazdina, 1984; Hrazdina *et al.*, 1987; Burbulis and Winkel-Shirley, 1999). Therefore, flavonoid monomers would be accumulated in the vacuolar storage pool (Debeaujon *et al.*, 2001) through different possible routes (i.e. tonoplast transport of 3′-*O*-epicatechin glucoside through MATE1; Zhao and Dixon, 2009). However, the mechanism of polymerization into condensed tannins remains totally unknown (Zhao *et al.*, 2010), while even the nature of precursor(s) remains hypothetical (Pang *et al.*, 2013). In any event, direct polymerization in the acid vacuolar sap would lead to a denaturation of vacuolar enzymes and tonoplast transporters by neoformed tannins. The model presented in this work describes a highly compartmented system for the polymerization of tannins: in fact, depending on the progress of the tannosome journey, the organelle is bound by one (the tannosome stage), two (the shuttle stage) and finally three (the vacuolar stage) membranes. Condensed tannins are permanently separated from proteins outside differentiating thylakoids, therefore preventing denaturation of these proteins, which would be lethal. The present model thus fits the prerequisite of Davies and Schwinn (2006) that 'Any enzymatic polymerization process would need to evolve a mechanism for avoidance of inhibitory–PA interactions'.

The role of chloroplasts in the synthesis of phenolics must not be overlooked: in fact, through its shikimate pathway (Herrmann,

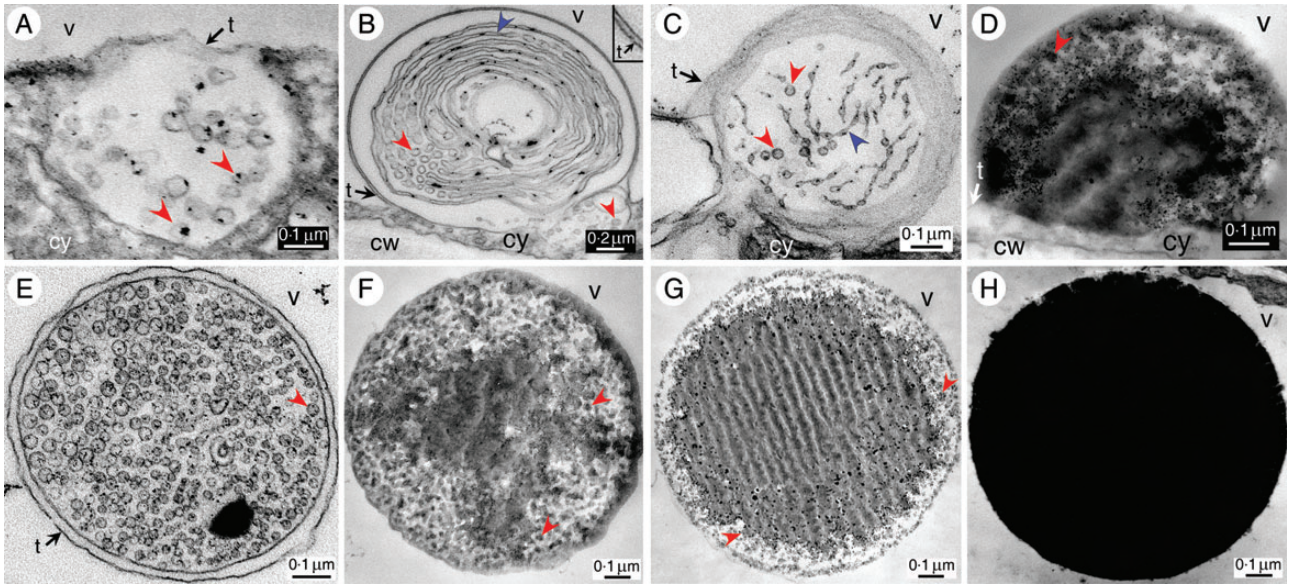

FIG. 5. (A–D) Entrance into the vacuole of shuttles (A) containing tannosomes, (B) containing coiled pearling thylakoids and tannosomes (the shuttle is bound by an inner membrane and a tonoplast portion as its outer membrane – insert, magnification of the two membranes), (C) with well constituted pearling thylakoids and tannosomes and (D) containing filling tannosomes. (E) A shuttle in the vacuole containing empty and filling tannosomes and bound by its membrane and a tonoplast ring. (F–H) Progressive filling of tannosomes inside shuttles. Abbreviations: cw, cell wall; cy, cytoplasm; t, tonoplast; v, vacuole.

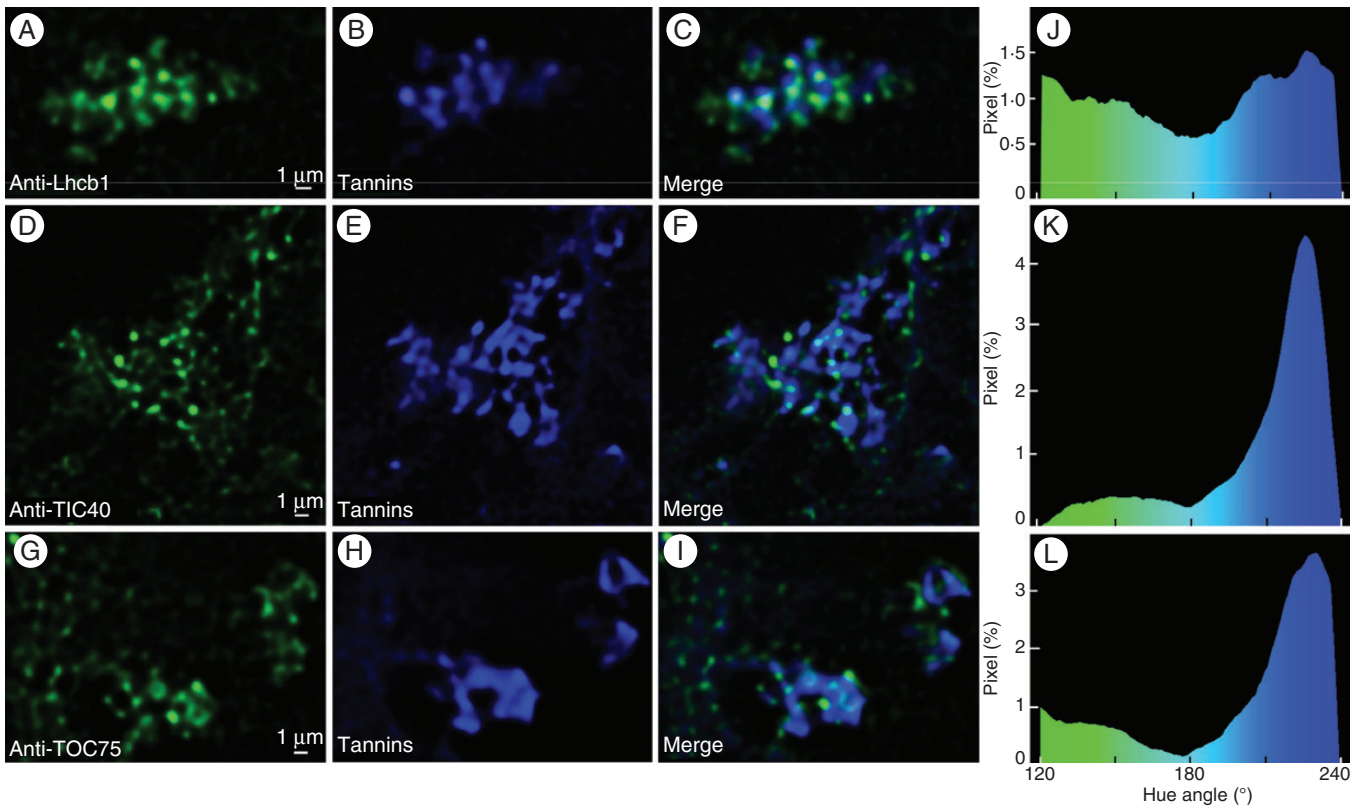

FIG. 6. Subcellular localization of LHCII type I chlorophyll *a/b*-binding protein (lhcb1), and translocon complex proteins from the inner (TIC 40) and outer (TOC 75) chloroplast envelopes, and tannins, in a *Vitis* cell. Confocal images showing clustered shuttles in the vacuole marked with (C) anti-Lhcb1, (G) anti-TIC40 and (J) anti-TOC75 antibodies and Alexa Fluor 633-conjugated rabbit secondary antibody, and (B, F, J) tannin autofluorescence; (C, F, I) merged images from (A, B), (D, E) and (G, H), respectively; (J–L) image analyses of (C, F, I), respectively, after thresholding, showing for each pixel (as percentage/total pixels), its hue angle (°).

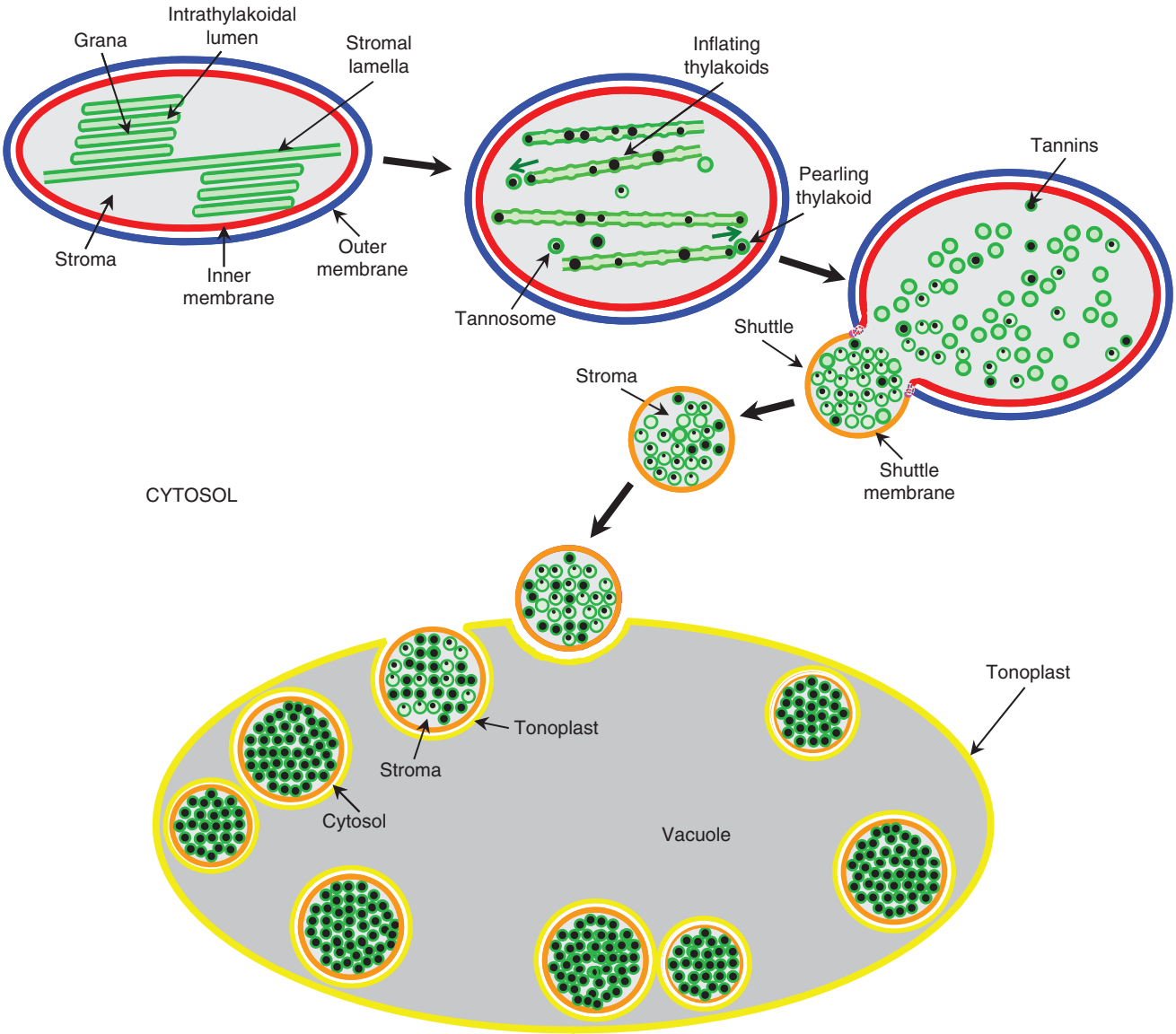

FIG. 7. Schematic of the time course of differentiation of chloroplast with unstacking and inflation of grana thylakoids, their pearling into tannosomes, the encapsulation of tannosomes into shuttles with progressive filling, their journey through the cytosol and their final storage in the vacuole. Not to scale.

1995), this organelle is the sole source of aromatic compounds in plant cells. Tian *et al.* (2008) reported a novel localization of chalcone synthase in the chloroplast; and, interestingly, this organelle has been repeatedly described as containing flavonoids [e.g catechin (Kefeli and Turetskaia, 1966; Liu *et al.*, 2009)] it has even been reported as having the capacity to synthesize *per se* flavonols (Zaprometov and Bukhlaeva, 1970; Saito, 1974; Saunders and McClure, 1976; Zaprometov and Nikolaeva, 2003) and catechin (Zaprometov, 1966; Zaprometov and Kolonkova, 1967). In the same vein, Chen *et al.* (2006) and Wang *et al.* (2010), respectively, reported plastidial localizations of cinnamate-4-hydroxylase (C4H) and anthocyanidin synthase (ANS). All these data converge on the chloroplast possessing the machinery for the synthesis of flavan-3-ols, possible precursors of condensed tannins.

Whatever the location of the tannosome (stroma, cytosol or vacuole), polymerization starts from the inner face of the thylakoidal membrane of the tannosome, synthesized material being pushed into the intrathylakoidal lumen until complete filling. This continuum can be viewed as a dynamic phenomenon: chlorophyllous shuttles progressively fill with tannins. Finally, the possibility exists that synthesis of monomers proceeds in the plastidial stroma or the stromal medium surrounding tannosomes in shuttles, polymerization occurring during active permeation of these precursors through the thylakoidal membrane of the tannosome with final storage in its lumen.

SUPPLEMENTARY DATA

Supplementary data are available online at www.aob.oxfordjournals.org and consist of the following. Figure S1: confocal images of controls of gelatin–Oregon Green on tannin-free plant materials. Figure S2: chloroplasts from *Vitis* mesocarp cells viewed by light and epifluorescence microscopy. Figure

S3: various aspects of tannosome shuttles from diverse plant divisions. Figure S4: epifluorescence micrographs of tannin accretions from diverse divisions.

ACKNOWLEDGEMENTS

We thank Dr Chantal Cazevieille and Cécile Sanchez [Centre de Ressources en Imagerie Cellulaire (CRIC), Université Montpellier I, Montpellier, France] and Elodie Jublanc (INRA, Montpellier, France) for their technical assistance in transmission electron and confocal microscopy, respectively. Thanks are also due to Marc Lartaud (PHIV, Montpellier, France) for processing confocal images, Dr Jean-François Briat (INRA-BPMP, Montpellier, France) and Professor Francis Marty for critical reading of the manuscript. Dr Mary Kelly (Faculty of Pharmacy, Montpellier, France) and the referees are also thanked for helping to make significant improvements to this paper.

LITERATURE CITED

Abrahams S, Lee E, Walker AR, Tanner GJ, Larkin PJ, Ashton AR. 2003. The *Arabidopsis TDS4* gene encodes leucoanthocyanidin dioxygenase (LDOX) and is essential for proanthocyanidin synthesis and vacuole development. *The Plant Journal* **35**: 624–636.

Berli FJ, Fanzone M, Piccoli P, Bottini R. 2011. Solar UV-B and ABA are involved in phenol metabolism of *Vitis vinifera* L. increasing biosynthesis of berry skin polyphenols. *Journal of Agricultural and Food Chemistry* **59**: 4874–4884.

Brillouet JM, Escoute J. 2012. A new technique for visualizing proanthocyanidins by light microscopy. *Biotechnic and Histochemistry* **87**: 195–200.

Burbulis IE, Winkel-Shirley B. 1999. Interactions among enzymes of the *Arabidopsis* flavonoid biosynthetic pathway. *Proceedings of the National Academy of Sciences, USA* **96**: 12929–12934.

Cadot Y, Miñana Castelló MT, Chevalier M. 2006. Flavan-3-ol compositional changes in grape berries (*Vitis vinifera* L. cv Cabernet Franc) before veraison, using two complementary analytical approaches, HPLC reversed phase and histochemistry. *Analytica Chimica Acta* **563**: 65–75.

Chafe SC, Durzan DJ. 1973. Tannin inclusions in cell suspension cultures of white spruce. *Planta* **113**: 251–262.

Chen J-Y, Wen P-F, Kong W-F, Pan O-H, Wan S-B, Huang W-D. 2006. Changes and subcellular localizations of the enzymes involved in phenylpropanoid metabolism during grape berry development. *Journal of Plant Physiology* **163**: 115–127.

Cohen SD, Tarara JM, Gambetta GA, Matthews MA, Kennedy JA. 2012. Impact of diurnal temperature variation on grape berry development, proanthocyanidin accumulation, and the expression of flavonoid pathway genes. *Journal of Experimental Botany* **63**: 2655–2665.

Constabel F. 1969. Über die Entwicklung von Gerbstoffzellen in Calluskulturen von *Juniperus communis* L. *Planta Medica* **17**: 101–115.

Davies K, Schwinn KE. 2006. Molecular biology and biotechnology of flavonoids biosynthesis. In: Andersen ØM, Markham KR. eds. *Flavonoids – chemistry, biochemistry and applications*. Boca Raton, FL: CRC Press, 143–218.

Debeaujon I, Peeters AJ, Leon-Kloosterziel KM, Koornneef M. 2001. The TRANSPARENT TESTA12 gene of *Arabidopsis* encodes a multidrug secondary transporter-like protein required for flavonoid sequestration in vacuoles of the seed coat endothelium. *The Plant Cell* **13**: 853–871.

Franck F, Juneau P, Popovic R. 2002. Resolution of the photosystem I and photosystem II contributions to chlorophyll fluorescence of intact leaves at room temperature. *Biochimica et Biophysica Acta* **1556**: 239–246.

Georgieva K, Sárvári É, Keresztes Á. 2010. Protection of thylakoids against combined light and drought by a luminal substance in the resurrection plant *Haberlea rhodopensis*. *Annals of Botany* **105**: 117–126.

Gifford EM, Stewart KD. 1968. Inclusions of the proplastids and vacuoles in the shoot apices of *Bryophyllum* and *Kalanchoë*. *American Journal of Botany* **55**: 206–279.

Hagerman AE, Butler HG. 1981. The specificity of proanthocyanidin–protein interactions. *Journal of Biological Chemistry* **256**: 4444–4497.

He J, Huang LK, Whitecross MI. 1994. Chloroplast ultrastructure changes in *Pisum sativum* associated with supplementary ultraviolet (UV-B) radiation. *Plant, Cell and Environment* **17**: 771–775.

Herrmann KM. 1995. The shikimate pathway: early steps in the biosynthesis of aromatic compounds. *The Plant Cell* **7**: 907–919.

Hrazdina G, Zobel AM, Hoch HC. 1987. Biochemical, immunological and immunocytochemical evidence for the association of chalcone synthase with endoplasmic reticulum membranes. *Proceedings of the National Academy of Sciences, USA* **84**: 8966–8970.

Jansen MAK, Gaba V, Greenberg BM. 1998. Higher plants and UV-B radiation: balancing damage, repair and acclimation. *Trends in Plant Science* **3**: 131–135.

Jodłowska S, Latała A. 2011. The comparison of spectrophotometric method and high-performance liquid chromatography in photosynthetic pigment analysis. *OnLine Journal of Biological Sciences* **11**: 63–69.

Juhász GD, Dános B, Rakován N. 1969. Licht- und elektronenmikroskopische Untersuchung gerbstoffhaltiger Zellen in den reproduktiven Organen der Cornus-arten. *Annales Universitatis Scientiarum Budapestinensis de Rolando Eotvos Nominatae Sectio Biologica* **12**: 158–161.

Kefeli VI, Turetskaia R. 1966. Localisation of natural phenolic inhibitors in cells of willow leaves. *Dokladi Akademii Nauk SSSR* **170**: 472–475.

Keresztes Á, Sárvári É. 2001. Investigations into the 'inverse contrast' of chloroplast thylakoids. *Acta Botanica Croatica* **60**: 253–265.

Kostina E, Wulff A, Julkunen-Tiitto R. 2001. Growth, structure, stomatal responses and secondary metabolites of birch seedlings (*Betula pendula*) under elevated UV-B radiation in the field. *Trees* **15**: 483–491.

Liu Y, Gao L, Xia T, Zhao L. 2009. Investigation of the site-specific accumulation of catechins in the tea plant [*Camellia sinensis* (L.) O. Kuntze] via vanillin-HCl staining. *Journal of Agricultural and Food Chemistry* **57**: 10371–10376.

Marchant R, Moore RT. 1973. Lomasomes and plasmalemmasomes in fungi. *Protoplasma* **76**: 235–247.

Michodjehoun-Mestres L, Souquet JM, Fulcrand H, Meudec E, Reynes M, Brillouet JM. 2009. Characterisation of highly polymerised prodelphinidins from skin and flesh of four cashew apple (*Anacardium occidentale* L.) genotypes. *Food Chemistry* **114**: 989–995.

Mueller WC, Beckman CH. 1976. Ultrastructure and development of phenolic-storing cells in cotton roots. *Canadian Journal of Botany* **54**: 2074–2082.

Mueller WC, Greenwood AD. 1978. The ultrastructure of phenolic-storing cells fixed with caffeine. *Journal of Experimental Botany* **29**: 757–764.

Pang Y, Cheng X, Huhman DV, *et al*. 2013. *Medicago* glucosyltransferase UGT72L1: potential roles in proanthocyanidin biosynthesis. *Planta* **238**: 139–154.

Parham RA, Kaustinen HM. 1977. On the site of tannin synthesis in plant cells. *Botanical Gazette* **138**: 465–467.

Reed HS, Dufrénoy J. 1942. Catechol aggregates in the vacuoles of cells of zinc deficient plants. *American Journal of Botany* **29**: 544–551.

Saito K. 1974. Possible site of flavonoid synthesis in the photosynthetic apparatus. *Biochemical Journal* **144**: 431–432.

Saslowsky D, Winkel-Shirley B. 2001. Localization of flavonoid enzymes in *Arabidopsis* roots. *The Plant Journal* **27**: 37–48.

Sato S, Adachi A, Sasaki Y, Ghazizadeh M. 2008. Oolong tea extract as a substitute for uranyl acetate in staining of ultrathin sections. *Journal of Microscopy* **229**: 17–20.

Saunders JA, McClure JW. 1976. The occurrence and photoregulation of flavonoids in barley plastids. *Phytochemistry* **15**: 623–626.

Selga M, Selga T. 1998. Interrelated transformations of chloroplast ultrastructure and morphogenesis of plants caused by UV-A radiation. In: Garab G. ed. *Photosynthesis: mechanism and effects.* Amsterdam: Kluwer Academic Publishers, 2413–2416.

Sironval C, Kirchman R, Bronchart R, Michel JM. 1968. Sur le freinage de l'accumulation des chlorophylles dans les feuilles primordiales de *Phaseolus vulgaris* L. var. Commodore à la suite d'une irradiation γ; photorestauration en lumière continue. *Photosynthetica* **2**: 57–67.

Souquet JM, Cheynier V, Brossaud F, Moutounet M. 1996. Polymeric proanthocyanidins from grape skins. *Phytochemistry* **43**: 509–512.

Stefanowska M, Kuraś M, Kacperska A. 2002. Low temperature-induced modifications in cell ultrastructure and localization of phenolics in winter oilseed rape (*Brassica napus* L. var. *oleifera* L.) leaves. *Annals of Botany* **90**: 637–645.

van Steveninck ME, van Steveninck RFM. 1980. Plastids with densely staining thylakoid contents in *Nymphoides indica*. II. Characterization of stainable substance. *Protoplasma* **103**: 343–360.

Tian L, Wan SB, Pan QH, Zheng YJ, Huang WD. 2008. A novel plastid localization of chalcone synthase in developing grape berry. *Plant Science* **175**: 431–436.

Treutter D. 1989. Chemical reaction detection of catechins and proanthocyanidins with 4 dimethylaminocinnamaldehyde. *Journal of Chromatography* **467**: 185–193.

Wagner GJ, Hrazdina G. 1984. Endoplasmic reticulum as a site of phenylpropanoid and flavonoid metabolism in *Hippeastrum*. *Plant Physiology* **74**: 901–906.

Wang H, Wang W, Li H, Zhang P, Zhan J, Huang W. 2010. Gene transcript accumulation, tissue and subcellular localization of anthocyanidin synthase (ANS) in developing grape berries. *Plant Science* **179**: 103–113.

Wardrop AB, Cronshaw J. 1962. Formation of phenolic substances in the ray parenchyma of angiosperms. *Nature* **193**: 90–92.

Whatley JM. 1971. The chloroplasts of *Equisetum telmateia* Erh.: a possible developmental sequence. *New Phytologist* **70**: 1095–1102.

Zaprometov MN. 1966. The rate of catechin formation in young shoots of tea plants. In: *Biochemistry and advanced technology of tea production*. Moscow: Nauka, 32–36.

Zaprometov MN, Bukhlaeva VY. 1970. The products of photosynthesis in Scots pine (*Pinus sylvestris* L.). *Soviet Plant Physiology* **17**: 277–279.

Zaprometov MN, Kolonkova SV. 1967. Biosynthesis of phenolic compounds in the chloroplast of tea plant. *Dokladi Akademii Nauk SSSR* **176**: 470–473.

Zaprometov MN, Nikolaeva TN. 2003. Chloroplasts isolated from kidney bean leaves are capable of phenolic compound biosynthesis. *Russian Journal of Plant Physiology* **50**: 623–626.

Zhao J, Dixon RA. 2009. MATE transporters facilitate vacuolar uptake of epicatechin 3'-*O*-glucoside for proanthocyanidin biosynthesis in *Medicago truncatula* and *Arabidopsis*. *The Plant Cell* **21**: 2323–2340.

Zhao J, Pang Y, Dixon RA. 2010. Update on biosynthesis of proanthocyanidins. The mysteries of proanthocyanidin transport and polymerization. *Plant Physiology* **153**: 437–443.